PCCP

Accepted Manuscript

Physical Chemistry Chemical Physics RSCPublishing

ARTICLE

Local Bias Induced Ferroelectricity in Manganites With Competing Charge and Orbital Order States

Cite this: DOI: 10.1039/x0xx00000x

Received 00th January 2013,
Accepted 00th January 2013

DOI: 10.1039/x0xx00000x

www.rsc.org/

Fábio G. N. Figueiras*[,a], Igor K. Bdikin[b], Vitor B. S. Amaral[a] and Andrei L. Kholkin[c]

Perovskite-type manganites, such as $Pr_{1-x}Ca_xMnO_3$, $La_{1-x}Ca_xMnO_3$ and $La_{1-x}Sr_xMnO_3$ solid solutions are set forth as case study of ferroelectricity formation mechanisms associated with the appearance of site- and bond-centered orbital ordering which breaks structural inversion symmetry. Even though the observation of macroscopic ferroelectricity may be hindered by the finite conductivity of manganites, polarization can still exist in nanoscale volumes. We use Piezoresponse Force Microscopy to probe local bias induced modifications of electrical and electromechanical properties at the manganites surface. Clear bias-induced piezocontrast and local hysteresis loops are observed in $La_{0.89}Sr_{0.11}MnO_3$ and $Pr_{0.60}Ca_{0.40}MnO_3$ compounds providing convincing evidences of the existence of locally induced polar states well above the transition temperature to CO phase, while the reference samples without CO behavior show no ferroelectric-like response. Such coexistence of ferroelectricity and magnetism in manganites due to the charge ordering (CO) under locally applied electric field opens up a new pathway to expand the phase diagrams of such systems and to achieve spatially localized multiferroic effects with a potential to be used in a new generation of memory cells and data processing circuits.

Introduction

Manganites present a wide spectrum of structural and functional phases [1,2] associated with the competing charge, lattice, orbital and spin degrees of freedom, and become an excellent test ground for materials modification. Multifunctional behavior can be achieved through careful chemical manipulation, resulting in colossal magneto resistance (CMR), ferroelectricity (FE), conductivity behavior, complex magnetic states and structural symmetries, [3,4] whereas various phase transitions can be induced by means of external factors (temperature, pressure, magnetic and electrical fields). [5,6] In the case of manganites possessing simultaneously charge and orbital order (CO/OO) properties, the occurrence of particular electronic spatial modulations (bond or spin dimerization) which present simultaneous site inequivalency and bond distortion, may allow breaking structural inversion symmetry potentially leading to ferroelectricity. [7,8] However, manganites generally present relatively low specific resistivity making conventional dielectric measurements not viable due to extensive conductivity loss. The estimated coexistence of such CO/OO states should in general have energy levels very close to one another and only found active at low temperatures in the conventional phase diagram; nonetheless, localized FE effects (10 nm scale) can be studied via Piezoresponse Force Microscopy (PFM) and particularly, bias lithography techniques can be used to induce phase transition in selected regions of the material surface. [9] In its turn, Band Excitation Piezoresponse Spectroscopy (BEPS) is a useful tool to testify and to quantify the presence of locally induced ferroelectricity, verify the possibility of charge accumulation or electrochemical phenomena; [10,11] in addition, current vs. voltage (***i-V***) probing enable to inspect charge carriers injection/mobility in the subsurface region..

The phase diagrams of $Pr_{1-x}Ca_xMnO_3$ [4], $La_{1-x}Sr_xMnO_3$ [11] and $La_{1-x}Ca_xMnO_3$ [3] manganites present for each system some particular doping compositions regions (in **x**) having rich transition thresholds between insulating and/or CO/OO properties states also correlated to Insulating-Metal transition and even magnetic ordered phases; these transitions are easily affected by external perturbations, and could reveal complex dielectric/ magnetic/ structural response behaviors. Inspiring research studies can be found in the work of Jooss, [13] which identifies localized bias induced structural transitions and introduces a further insight into the $Pr_{1-x}Ca_xMnO_3$ system, extending for $0.3 < \mathbf{x} < 0.5$, having simultaneous charge and antiferromagnetic orders below $\mathbf{T}_N$, imposing a cooperative Jahn-Teller (JT) distortions leading to a non-centrosymmetric $P2_1nm$ structure, hence meeting some of the requisites to be classified as an intrinsic type *I* multiferroic and making it one of the best candidates to prove a promising model of induced FE effects in manganites. In addition, electric field gradient (EFG) studies of A. Lopes et al. [14] across the $Pr_{1-x}Ca_xMnO_3$ phase diagram, using hyperfine Perturbed Angular Correlations (PAC) measurements with ^{111m}Cd, revealed typical signatures of a phase transition involving long-range ordering of local dipoles over the entire CO/OO region. Previous bias lithography and PFM experiments performed in a single crystal $La_{0.89}Sr_{0.11}MnO_3$ sample provide also a reference for this study. [15] FE localized phenomena is an important scientific promise for creating artificial multiferroic materials and memory states.

Experimental

A selection of manganites samples having compositions near CO/OO transitions thresholds and also some without CO/OO (control) samples, [11,16] includes single crystals prepared by floating zone method and of polycrystals prepared by solid state process, comprise $La_{1-x}Sr_xMnO_3$ (x = 0.11, 0.30), $Pr_{1-x}Ca_xMnO_3$ (x = 0.00, 0.35, 0.40, 0.85) and $La_{1-x}Ca_xMnO_3$ (x = 0.05; 0.33). Experiments were performed using several PFM systems including *Asylum*®, *PicoPlusTM*®, *Agilent*®, *NT-MDT*® and *Veeco*®; general procedure consists in selecting a 5x5 μm region with regular topology, then to sketch a lithographic frame of 2 μm length separated lines traced at ~100 nm/s at different bias voltages (up to ±30 Vd.c.), as schematized in figure 1. Tip pressure is adjusted to avoid scratching the surface while maximizing electrical contact. Further BEPS mapping, piezocontrast imaging, localized piezo-response loops, and *i-V* curves measurements between ±10 Vd.c. (up to 20 nA detection maximum), enable to trace particular effects to stimulated regions.

Results and discussion

Extensive lithographic experiments and PFM measurements were carried out in the several samples; in general, subsequent to the bias lithographic tests, topological mapping show no relevant mechanical deformation of the surface; enabling to discriminate the piezoresponse contrast that appears in the respective lithographed paths from topological cross-talk effects. Graphs of figure 2a and 2b enable to abridge typical piezoresponse loops averaged from the regions subjected to local poling in comparison to the non-stimulated areas. BEPS measurements gather a widespread sequence of amplitude and phase data obtained for each pixel as function of the probing frequency and bias voltage, this method enables data acquisition having unambiguous decoupling of the conservative and dissipative interactions, removing topographic cross-talk and allowing identification of non-linear responses. The contours and contrasts found in the set of parameters maps depicted in the BEPS measurements of figures 3 and 4 can be interpreted as the change in behavior of the loops profiles within the bias lithographed regions compared to the non-stimulated surface, inferred from charting nucleation sites, energy dissipation on polarization switching, saturation (R±) and coercive (V±) FE parameters. [10]
In figure 3 are shown PFM and BEPS scans performed in a $Pr_{0.60}Ca_{0.40}MnO_3$ sample measured at room temperature in the paramagnetic phase and above the CO/OO transition.

Experimental lithographic bias lines poling at +10 and -10 V gave rise to opposite piezoelectric contrast, evidencing the formation of a local polar state, without visible effects on the sample' surface topography. The polarization relaxes after a few hours, a time scale much longer than the expected for transient trapped charges.
The experiments performed in the $La_{0.89}Sr_{0.11}MnO_3$ monocrystalline sample, the PFM scans of figure 4 testify how local piezoresponse signals are directly traceable to the lithographic paths stimulated regions. It is possible to observe that the lithographic paths made under negative bias voltage induce stronger piezoresponse contrast on the sample surface than the positive bias; such asymmetric response of the sample is coherent with the ***i-V*** experiments further discussed. No reaction was detected from the +10 $V_{d.c.}$ litho path; a minor surface alteration can be detected at the end of the path made at -10 $V_{d.c.}$ due to incidental parking of the tip and should not be considered relevant, since the bulging is not extended to the rest of the stimulated region.
For the other manganite samples having compositions that also allow CO/OO states, namely the nominal $Pr_{0.65}Ca_{0.35}MnO_3$, $Pr_{0.15}Ca_{0.85}MnO_3$ and $La_{0.05}Ca_{0.95}MnO_3$, respective PFM measurements reveal some circumspect piezoresponse contrast traceable mainly to the negative lithographic paths, not enough to be considered as substantial BEPS results to be shown, nevertheless, some details are worth notice. The monocrystalline $Pr_{0.65}Ca_{0.35}MnO_3$ sample does not have reaction to lithographic bias fields smaller than |±20| $V_{d.c.}$; some scarce surface bulging from the tip passage at -20 $V_{d.c.}$ could be observed, nevertheless the piezoresponse amplitude contrast is homogeneous along all the path, enabling again to discard cross talk interference, hence attesting the correlation to a change in the dielectric properties and not due to mechanical/chemical features; for the +20 $V_{d.c.}$ litho path the piezoresponse amplitude changes signal, pointing again to poling effects on the material. For these two samples the respective CO/OO states lie at a lower temperature (T_{CO} ~210 K for x = 0.35 and $\mathbf{T}_N$ = 120 K for x = 0.85) both are chemically much closer to the paraelectric composition threshold (x = 0.3 and x = 0.9 respectively), hence metastable ordered states become easily dispersed by room temperature thermodynamic conditions.
For the $La_{0.95}Ca_{0.05}MnO_3$ sample the piezocontrast observed over the stimulated regions is essentially due to a signal phase shift without significant amplitude increase in comparison to the non-stimulated regions. These alterations of dielectric properties is only partially revealed in BEPS maps, but not attaining such clear switching and saturation parameters such as described for the $Pr_{0.60}Ca_{0.40}MnO_3$ and $La_{0.89}Sr_{0.11}MnO_3$ samples.

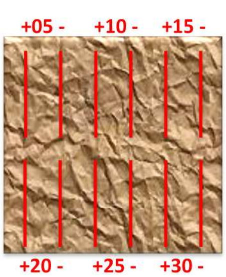

Fig. 1: Schematic of lithographic bias paths in a 5x5 μm² of samples surface.

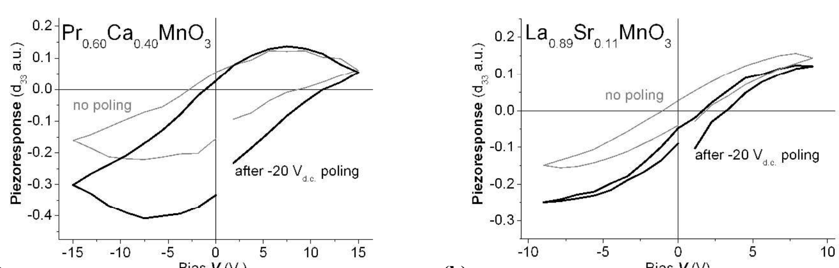

Fig. 2: Comparison between typical pieoezoresponse loops from the distinct regions of the: (a) $Pr_{0.60}Ca_{0.40}MnO_3$, and (b) $La_{0.89}Sr_{0.11}MnO_3$ samples, before and after poling bias lithography.

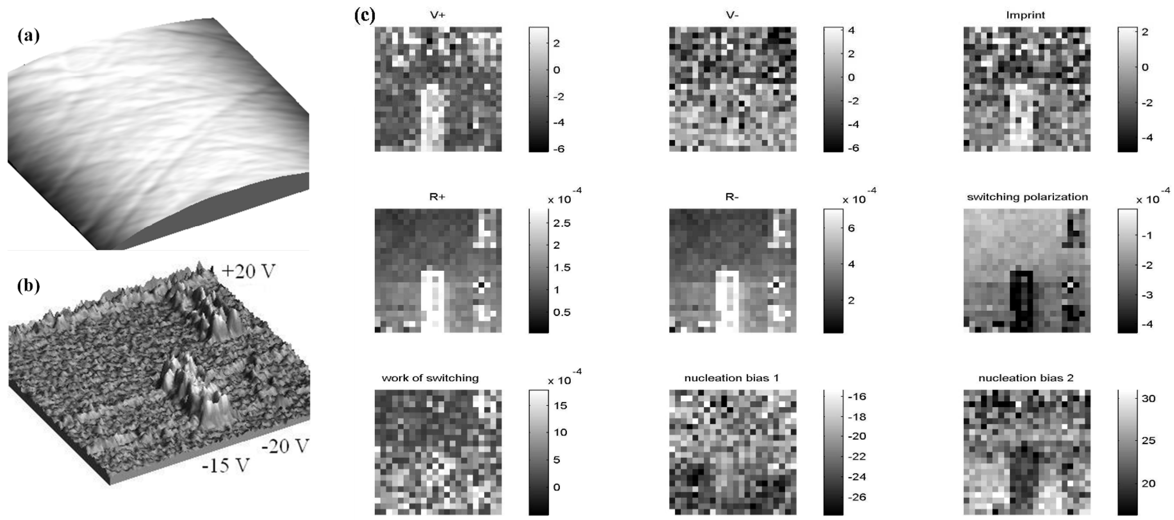

Fig. 3: Topographic (a) and piezo contrast (b) scans of 3x3 μm^2 surface after performing bias lithographic paths; detail of the respective BEPS maps results (c) for the single crystal $Pr_{0.60}Ca_{0.40}MnO_3$ sample.

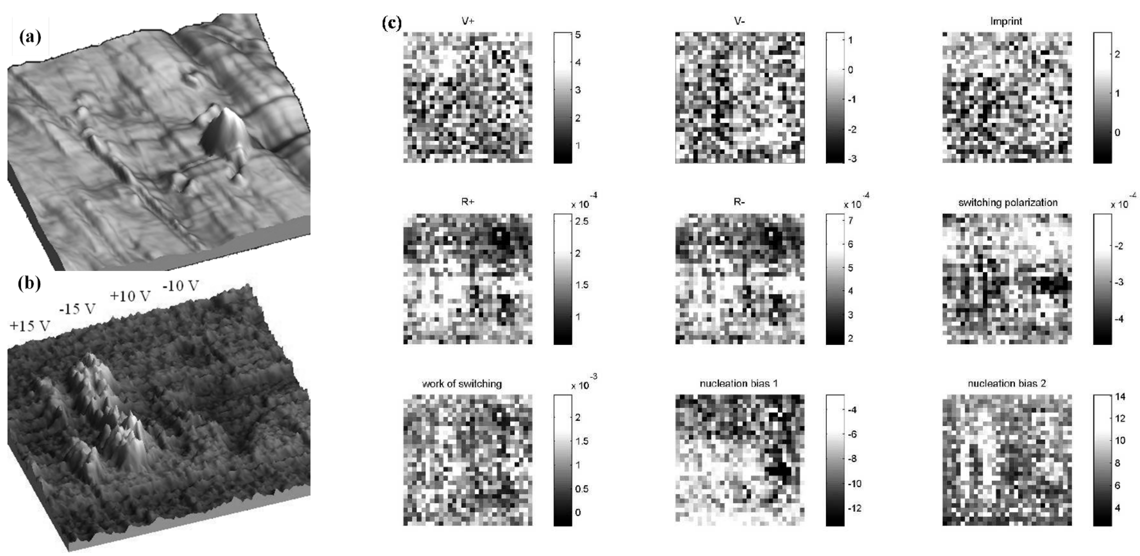

Fig. 4: Topographic (a) and piezo contrast (b) scans of 3x3 μm^2 surface after performing bias lithographic paths; detail of the respective BEPS maps results (c) for the single crystal $La_{0.89}Sr_{0.11}MnO_3$ sample.

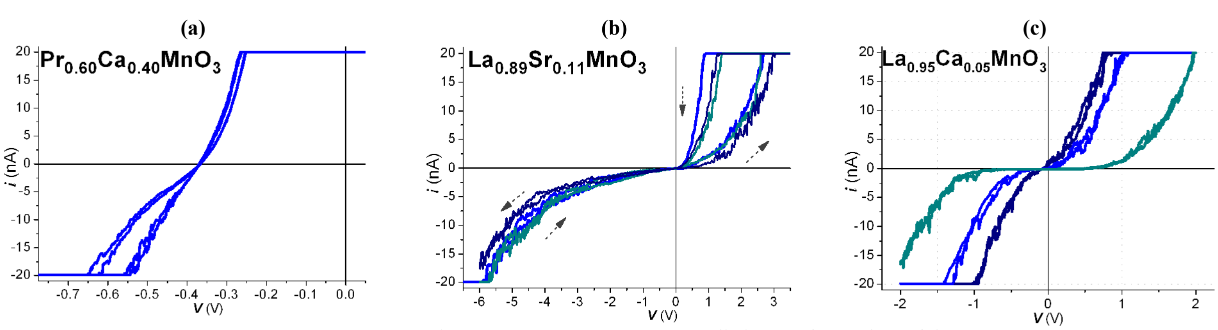

Fig. 5: Representative ***i-V*** curves measurements at distinct surface points of the $Pr_{0.60}Ca_{0.40}MnO_3$ (a), $La_{0.89}Sr_{0.11}MnO_3$ (b), and $La_{0.95}Ca_{0.05}MnO_3$ (c) samples.

The symmetric behavior of the ***i-V*** curves shown in figure 5(c) suggests more conventional low conductivity phenomena.

Most pertinent fact is that equivalent bias lithographic tests (up to ±30 $V_{d.c.}$) performed in conventional dielectric oxides like Mn_3O_4 or $PrMnO_3$, $La_{0.67}Ca_{0.33}MnO_3$ and $La_{0.7}Sr_{0.3}MnO_3$ manganites did not lead to any piezoresponse signal or BEPS contrast maps. These complementary observations in the reference compounds suggest that possible capacitive effects or electrochemical surface reaction promoted by the highly localized and intense electrical field, [17,**Error! Reference source not found.**] might not be the only phenomena accountable for the responses described in samples $Pr_{0.60}Ca_{0.40}MnO_3$ and $La_{0.89}Sr_{0.11}MnO_3$.

The reckonable local alterations of the dielectric properties of these CO/OO series of manganite samples under the lithographic bias stimulation do not follow conventional Ohm' law [18] neither Frenkel' law [19] where an increase in conductivity could be expected from lowering the carriers' activation energy when applying an electric field. In fact, higher electric conductivity manganite control samples such as $La_{0.67}Ca_{0.33}MnO_3$ renders any charge accumulation induced by the PFM tip to be rapidly dispersed in the material and dissipated through the sample holder electrode.

Some additional insight over the local effect of the bias poling upon the samples' surface state can be perceived from ***i-V*** probing measurements. [20] The relatively high resistivity found at the surface of the CO/OO type manganites series of samples (>10^3 Ω.mm), restricted the experimental conditions within distances of few μm between tip and sample holder electrode across the sample surface. Measurements are performed at 0.1 Hz ramps between ±10 V in order to establish a quantifiable current (0.1 nA < ***i*** < 20 nA), as well as to distinguish and to prevent inconsistent pA charge/discharge loops arising from an undesirable equivalent capacitor circuit from the system setup.

The ***i-V*** measurements were repeated at several points of the samples surface of which most consistent and representative results are shown in the graphs of figure 5. The reproducibility and number of cycles through the curves has certain limitations due to progressive tip wearing and degradation of sample surface as expected from to mechanical stress and current leakage/heating in addition to other hampering factors like surface inhomogeneities and hydration adsorbed layer.

An important trend that can be observed for the $Pr_{0.60}Ca_{0.40}MnO_3$ and $La_{0.89}Sr_{0.11}MnO_3$ samples is the asymmetric shape and hysteresis of the current response to the applied bias voltage in contrast to the symmetric behavior described for normal metal-manganite heterojunctions. [20] These asymmetries are revealed in the delay of current response to low negative bias voltage which can be related to the different availability and mobility of the charge carriers, electrons (polarons) or holes in the material; reminding a semiconductor p-n junction and a Zener like effect. In its turn, the current inversion hysteresis can be associated to the FE domains inversion; in fact, the initial set of the bias probe voltage has a resolute influence in the outcome of the ***i-V*** measurements. When starting from -10 V the point effect on the sample surface can induce a localized FE state transition which leads to a dielectric behavior (no current flow) setting through the ramp up to +10 V; whereas starting from +10 V enables current flow and we observe a finite number of t ***i-V*** curves as testified in the respective left and center graphs of figure 5.

These expressive PFM sets of results are an indication that as well as local electrochemical oxygen diffusion phenomena, there can be also envolved additional mechanisms, in particular for manganite systems possessing CO/OO states. The highly confined electric field and a partial injection and trapping of charge carriers can reorganize the local polaronic distribution (modulated strain/electron/spin), [21] usually found in thermodynamic disarray at room temperature, hence promote the expansion of particular metastable state which can be detected by a dielectric/ferroelectric signature in contrast with the electrical properties of the conventional host phase.[22,23,24] The formation of these embedded charge/orbital and antiferromagnetic orders prevent electron hopping and the correlations can survive locally as "Zener polarons" [25,26] above $\mathbf{T}_{CO}$ and even $\mathbf{T}_{N}$. Under this circumstances Mn ions and Mn-O-Mn bonds become nonequivalent resulting a noncentrosymmetric electronic structure which is prone to exhibit some piezoelectric response.

Conclusions

The present PFM studies performed at room temperature demonstrated that by means of suitable bias lithography stimulation, it is possible to induce and stabilize localized states which exhibit a clear piezocontrast, possibly associated with the presence of nanoscopic CO/OO regions beyond the thermodynamic conditions of the conventional phase diagram. SPM methods can be extended to variables such as magnetic and electric properties, temperature and time responses; combined with other local probe techniques like hyperfine spectroscopies and theoretical modeling, it can bring new insights on correlated electrons systems, opening new pathways to study local scale multiferroic phenomena originated on complex charge/orbital ordering effects in materials particularly susceptible to phase transitions under localized disturbance. Understanding the mechanisms that underlie such complex processes along with optimizing the technical procedures and materials design in order to reach room temperature stabilization of the modifications, ultimately lead to the design of artificial multiferroic materials and memory cells.

Acknowledgements

FCT and COMPETE/FEDER support through project PTDC/FIS/105416/2008 MULTIFOX and PEst-C/CTM/LA0011/2013, Grants SFRH/BD/25011/2005 and SFRH/BPD/80663/2011; ONRL CNMS proposal CNMS2009-083, with personal thanks to S. Kalinin, P. Maksymovych, S. Guo, K. Seal, S. Jesse, N. Balke and M. Nikiforov.

The autors also acknowledge Y. Tokura for the supply of the single crystal Pr-Ca manganite samples and P.B. Tavares for the La-Ca manganites.

Notes and references

[a] Physics Department & CICECO,
University of Aveiro, 3810-193 Aveiro, Portugal.
Fax: +351 234 401 470; Tel: +351 234 372 571;
*E-mail: ffigueiras@ua.pt
[b] Mechanics Eng. Department & TEMA, University of Aveiro, 3810-193 Aveiro, Portugal. Fax: + 351 234 370 953; Tel: +351 234 370 830
[c] Materials Eng. Ceramics Department & CICECO,
University of Aveiro, 3810-193 Aveiro, Portugal.

† Electronic Supplementary Information (ESI) available: [gray scale contrast version of coloured figures 3 and 4 found in online version]. See DOI: 10.1039/b000000x/

1 J. M. D. Coey, M. Viret and S. von Molnar, Adv. In Phys. 1999, **48**, 2, 167.
2 J. B. Goodenough, Handbook on the Physics and Chemistry of Rare Earths, 2003, **33**, Chapter 214, 249-351.
3 C. Martin, A. Maignan, M. Hervieu, and B. Raveau, Phys. Rev. B, 1999, **60**, 17.
4 Y. Tokura, Rep. Prog. Phys. 2006, **69**, 797.
5 E. Dagotto, T. Hotta, A. Moreo, Physics Reports, 2001, **344**, 1-153.
6 Y. Tomioka, A. Asamitsu, H. Kuwahara, Y. Moritomo and Y. Tokura, Phys. Rev. B, 1996, **53**, R1689-R1692.
7 J. Van Den Brink and D I. Khomskii, J. Phys.: Condens. Matter, 2008, **20**, 434217.
8 D. V Efremov, J. Van Den Brink and D. I. Khomskii, Nature Materials, 2004, **3**, 853-856.
9 S. V. Kalilin, et al., Mat. Today, 2008, **11**, 11, 16-27.
10 S. Jesse, Ho N. Lee, and S. V. Kalinin, Rev. Sci. Instrum. 2006, **77**, 073702, 77-86.
11 S. V. Kalinin, A. Borisevich, D. Fong, ACS Nano, 2012, **6** (12) 10423-10437.
12 A. Urushibara, Y. Moritomo, A Asamitsu, G. Kido, Y. Tokura, Phys. Rev. B, 1995, **51**, 14103.
13 Ch. Jooss, et al., PNAS, 2007, **104**, 34, 13597-13602.
14 A. M. L. Lopes, J. P. Araújo, V. S. Amaral, J. G. Correia, Y. Tomioka and Y. Tokura, Phys. Rev. Lett. 2008, **100**, 155702.
15 R. F. Mamin, I. K. Bdikin and A. L. Kholkin, App. Phys. Lett. 2009, **94**, 222901.
16 Asamitsu, Y. Tomioka, H. Kuwahara and Y. Tokura, Nature, 1997, **388**, 50-52.
17 M. Cherry, M. S. Islam and C. R. A. Catlow, Journal of Solid State Chemistry, 1995, **118**, 125-132.
18 N. I. Solin, A. A. Samokhvalov, and S. V. Naumov, Physics of the Solid State, 1998, **40**, 10, 1706-1709.
19 Ya. I. Frenkel', Zh. Éksp. Teor. Fiz. 1971, 8, 1292.
20 N. A. Tulina, S. A. Zverkov, A. Arsenov, Y. M. Mukovskii, D. A. Shulyatev, Physica C, 2003, **385**, 563–567.
21 K. H. Ahn, T. Lookman and A. R. Bishop, Nature, 2004, **428**, 401-404.
22 A. Sergienko, C. Sen and E. Dagotto, Phys. Rev. Lett. 2006, 97, 227204.
23 N. Panwar, I. K. Bdikin, A. N. Morozovska, and A. L. Kholkin, J. Appl. Phys. 2012, **112**, 052019.
24 N. Panwar, I. Coondoo, A.L. Kholkin, Solid State Comm. 2013, **164**, 38–41.
25 L. Wu, R. F. Klie, Y. Zhu and Ch. Jooss, Phys. Rev. B, 2007, **76**, 174210.
26 T. Mizokawa, Nanoscale Research Letters 2012, **7**, 582.